Title

Formation of Organic Acids and Carbonyl Compounds in n-Butane Oxidation via γ-Ketohydroperoxide Decomposition

Journal

Angewandte Chemie International Edition, 61(42)

ISSN

1433-7851

Authors

Popolan-Vaida, Denisia M

Eskola, Arkke J

Rotavera, Brandon

et al.

Publication Date

2022-10-17

DOI

10.1002/anie.202209168

Peer reviewed

How to cite: *Angew. Chem. Int. Ed.* **2022,** *61,* e202209168
International Edition: doi.org/10.1002/anie.202209168
German Edition: doi.org/10.1002/ange.202209168

Hydrocarbon Oxidation

Formation of Organic Acids and Carbonyl Compounds in *n*-Butane Oxidation via γ-Ketohydroperoxide Decomposition

Denisia M. Popolan-Vaida[+], Arkke J. Eskola[+], Brandon Rotavera, Jessica F. Lockyear, Zhandong Wang, S. Mani Sarathy, Rebecca L. Caravan, Judit Zádor, Leonid Sheps, Arnas Lucassen, Kai Moshammer, Philippe Dagaut, David L. Osborn, Nils Hansen, Stephen R. Leone,* and Craig A. Taatjes**

Abstract: A crucial chain-branching step in autoignition is the decomposition of ketohydroperoxides (KHP) to form an oxy radical and OH. Other pathways compete with chain-branching, such as "Korcek" dissociation of γ-KHP to a carbonyl and an acid. Here we characterize the formation of a γ-KHP and its decomposition to formic acid + acetone products from observations of *n*-butane oxidation in two complementary experiments. In jet-stirred reactor measurements, KHP is observed above 590 K. The KHP concentration decreases with increasing temperature, whereas formic acid and acetone products increase. Observation of characteristic isotopologs acetone-d_3 and formic acid-d_0 in the oxidation of $CH_3CD_2CD_2CH_3$ is consistent with a Korcek mechanism. In laser-initiated oxidation experiments of *n*-butane, formic acid and acetone are produced on the timescale of KHP removal. Modelling the time-resolved production of formic acid provides an estimated upper limit of 2 s^{-1} for the rate coefficient of KHP decomposition to formic acid + acetone.

Autoignition of hydrocarbon-air mixtures plays a crucial role in the development of new low-emission, high efficiency engine technologies[1] and relies on chain-branching reactions, which at low temperature (< 700 K) are largely initiated by reactions of carbon-centered hydroperoxyalkyl radicals (QOOH) with O_2. QOOH radicals are formed in a reaction sequence beginning with organic radicals (R) reacting with O_2 to form alkylperoxy radicals (RO_2) that subsequently isomerize to QOOH.[2] Addition of O_2 to a QOOH radical leads to an oxygen-centered OOQOOH radical, which can isomerize via a second intramolecular hydrogen transfer to the peroxy moiety (α to the hydroperoxy moiety), creating an essentially unbound carbon-centered radical with two hydroperoxy (–OOH) functional groups. This radical nearly immediately dissociates to ketohydroperoxide (KHP) + OH via O–O bond scission. Subsequent decomposition of the KHP into a second OH and an oxy radical governs low-temperature chain-branching. In the conventional alkane oxidation paradigm,[3] this had been the only dissociation pathway for KHP. However, it has recently been recognized that other channels can compete with this chain-branching step, for example, the

[*] Prof. D. M. Popolan-Vaida,[+] Dr. J. F. Lockyear, Prof. S. R. Leone
Department of Chemistry and Physics, University of California, Berkeley
Berkeley, CA 94720 (USA)
E-mail: denisia.popolan-vaida@ucf.edu
srl@berkeley.edu

Prof. D. M. Popolan-Vaida[+]
Department of Chemistry, University of Central Florida
Orlando, FL 32816 (USA)

Dr. A. J. Eskola,[+] Prof. B. Rotavera, Dr. R. L. Caravan, Dr. J. Zádor, Dr. L. Sheps, Dr. A. Lucassen, Dr. K. Moshammer, Dr. D. L. Osborn, Dr. N. Hansen, Dr. C. A. Taatjes
Combustion Research Facility, Sandia National Laboratories
Livermore, CA 94551 (USA)
E-mail: cataatj@sandia.gov

Dr. A. J. Eskola[+]
Department of Chemistry, University of Helsinki
00014 Helsinki (Finland)

Prof. B. Rotavera
Department of Chemistry and College of Engineering, University of Georgia
Athens, GA 30602 (USA)

Prof. Z. Wang, Prof. S. M. Sarathy
King Abdullah University of Science and Technology (KAUST), Clean Combustion Research Center (CCRC)
Thuwal 23955-6900 (Saudi Arabia)

Prof. Z. Wang
National Synchrotron Radiation Laboratory, University of Science and Technology of China
Hefei, Anhui 230029 (P. R. China)

Dr. R. L. Caravan
Chemical Sciences and Engineering Division, Argonne National Laboratory
Lemont, IL 60439 (USA)

Dr. A. Lucassen, Dr. K. Moshammer
Physikalisch-Technische Bundesanstalt
38116 Braunschweig (Germany)

Dr. P. Dagaut
Centre National de la Recherche Scientifique (CNRS), INSIS, ICARE
45071 Orléans Cedex 2 (France)

[+] These authors contributed equally to this work.

Korcek reaction,[4] in which decomposition of γ-KHP forms acid and carbonyl products, as described by Jalan et al.[5] Formation of acid products in some systems has since been attributed to KHP decomposition,[6] but despite strong circumstantial evidence, a definitive experimental assignment of the Korcek mechanism is lacking in the gas phase. The present work employs isotopic labeling to link two of the products of Korcek decomposition and furthermore uses time-resolved kinetics experiments to constrain the rate coefficient for a specific acid + ketone pathway.

KHP intermediates were characterized in hexane, heptane and dodecane oxidation years ago by gas chromatography and direct-injection mass spectrometry,[7] and are known to play a key role in tropospheric oxidation as well as in autoignition chemistry. Battin-Leclerc et al.[8] detected KHPs in *n*-butane oxidation experiments by using a jet-stirred reactor (JSR) and photoionization mass spectrometry. Using a multiplexed photo-ionization mass spectrometry (MPIMS) apparatus combined with a high-pressure reactor, Eskola et al.[9] studied the kinetics of KHP formation and decay in laser-initiated Cl oxidation of *n*-butane at 1–2 atm pressure and confirmed the photoionization spectrum of the KHP reported by Battin-Leclerc.[8] KHPs have also been recently observed and quantified in various synchrotron based photoionization mass spectrometry experiments.[6,10]

Jalan et al.,[5] in their study of the Korcek decomposition channel, performed detailed ab initio calculations of rate coefficients for KHP produced in propane oxidation. Goldsmith et al.[11] calculated the effect of residual excitation from the exothermicity of KHP formation on the pressure dependent rate coefficients for KHP decomposition in propane oxidation. Ranzi and co-workers[12] have reported calculations for KHP reactions in the *n*-butane oxidation system. Their results show a facile isomerization of γ-KHP to a cyclic peroxide intermediate (CPI) that further isomerizes via intramolecular hydrogen transfer, finally decomposing to organic acid + carbonyl products (referred to herein as a Korcek pair). Besides the importance of KHP decomposition in modeling fundamental autoignition chemistry, acid formation is of significance in both spark-ignition and compression ignition engines.[13]

Herbinet et al.[14] measured *n*-butane oxidation and employed a detailed chemical kinetics model to simulate mole fractions for many of the detected species. Apart from detecting acetic acid, formic acid, and other species that had been undetected in previous experiments on *n*-butane oxidation, they observed substantial acetone formation, two orders of magnitude above modeled acetone concentrations. However, neither formic acid nor acetic acid was considered in the *n*-butane oxidation kinetic model. The inability to model the experimentally observed organic acids and carbonyl species[14] reflects substantial uncertainty in the main formation channels and related kinetic parameters.

In the present work, two complementary experimental techniques were used to investigate low-temperature oxidation of normal and isotopically labeled *n*-butane: a steady-state jet-stirred-reactor (JSR, thermal ignition) combined with high-resolution synchrotron photoionization reflection time-of-flight molecular beam mass spectrometry (TOF-MBMS)[6] and a laser-initiated kinetic multiplexed (synchrotron) photoionization mass spectrometry (MPIMS)[15] apparatus interfaced with a high-pressure flow tube reactor.

The photoionization spectrum at *m/z* 104.047, corresponding to the ketohydroperoxide ($C_4H_8O_3$) species, was measured in the JSR *n*-butane oxidation experiments at ≈590 K and 740 Torr (see Figure 1). The photoionization spectrum agrees with earlier KHP spectra from measurements of *n*-butane oxidation by Battin-Leclerc et al.[8] and Eskola et al.[9] In the latter study, the dominant KHP observed in *n*-butane oxidation is identified as 3-hydroperoxybutanal, derived initially from *n*-butyl + O_2 followed by the 4-hydroperoxy-2-butyl + O_2 reaction (see Scheme S1). Therefore, the spectra in Figure 1 are assigned to 3-hydroperoxybutanal. The present work focuses on the Korcek decomposition of 3-hydroperoxybutanal to the formic acid/acetone pair, both of which were observed in the JSR and MPIMS experiments. This pair was selected for further study using comprehensive chemical kinetics modeling that show the channel leading to acetone + formic acid is expected to have a higher yield than the acetaldehyde + acetic acid channel, due to the lower barrier for cyclic intermediate decomposition.[5] All of the expected Korcek decomposition products, i.e., acetone, formic acid, acetaldehyde, and acetic acid, were detected in the JSR experiment. Figure 2 shows the temperature dependence of the observed KHP and its decomposition product signals from *n*-butane oxidation JSR experiments. Figure 2 also shows the *m/z* 86.037 ($C_4H_6O_2$) product that originates either from direct elimination of water from KHP or from loss of OH followed by reaction of the oxy radical co-product with O_2 ($HCOCH_2CH(O^{\bullet})CH_3 + O_2 \rightarrow HCOCH_2C(O)CH_3 + HO_2$). Because absolute photoionization cross sections are not available for the KHP or for the product at

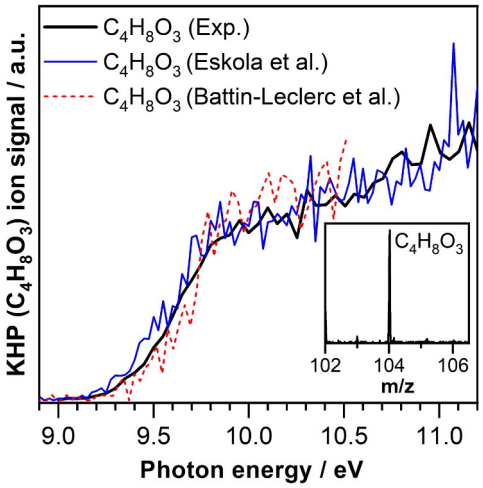

Figure 1. Photoionization spectrum of KHP ($C_4H_8O_3$), identified as 3-hydroperoxybutanal,[9] measured at ≈590 K, 740 Torr and compared with spectra from Eskola et al.[9] and Battin-Leclerc et al.[8] The insert represents the typical $C_4H_8O_3$ mass signal recorded at a photon energy of 10.5 eV.

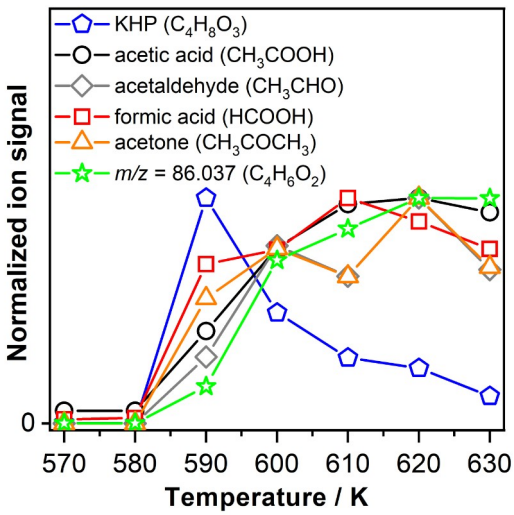

Figure 2. Temperature dependence of KHP and possible decomposition products (normalized to peak), resulted from channels other than the chain-branching (OH + oxy radical decomposition) step, measured in JSR *n*-butane oxidation experiments near 1 atm; residence time = 3.4 s, equivalence ratio = 1.0. The temperature of the maximum KHP is set to 590 K to match the observations of Battin-Leclerc et al.[8] See text and Supporting Information for more details.

m/z 86.037, the signals are normalized to the peak signal. An abrupt increase in KHP signal is evident near the lowest temperatures where significant oxidation occurs in the JSR. At ≈590 K, the KHP signal reaches its maximum and is reduced as temperature is increased. The signals from the possible KHP decomposition products increase with temperature over the same range that KHP decreases with temperature, consistent with the assumption that these stable species are products of KHP decomposition. However, in the global oxidation process of the JSR experiments, which involve long timescales, other pathways may also form these products.

To further constrain the experimental observation of the Korcek decomposition mechanism, oxidation of $CH_3CD_2CD_2CH_3$ was carried out in the JSR at ≈600 K. The oxidation of this selectively deuterated *n*-butane is expected to produce HCOOH and acetone-d_3 via Korcek decomposition of KHP-d_3, as shown in Scheme 1. Because formation of acetone-d_3 requires either a CD_3 group or deuterium substitution on non-adjacent carbons, no other pathways are likely to produce it in $CH_3CD_2CD_2CH_3$ oxidation. The

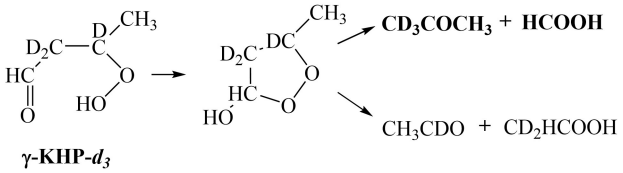

Scheme 1. Decomposition of 3-hydroperoxybutanal-d_3 (γ-KHP-d_3) into carbonyl + acid pairs via the Korcek mechanism. 3-hydroperoxybutanal-d_3 is the main KHP observed in *n*-butane-d_4 oxidation. The Korcek pathway observed in this study is indicated in bold.

detection of acetone-d_3 represents a strong indication for a KHP Korcek decomposition mechanism. The contribution of reaction channels ($OH + CH_2O \rightarrow H + HCOOH$ and $OH + CH_3CHO \rightarrow CH_3 + HCOOH$) other than Korcek that might produce formic acid-d_0 in the $CH_3CD_2CD_2CH_3$ oxidation are estimated to be negligible based on the rate constants and concentrations of the precursors of these reactions at 600 K (see Section 2, Supporting Information). Figure 3 shows the measured photoionization spectra of the (a) *m/z* 61.061, and (b) *m/z* 46.005 products observed in $CH_3CD_2CD_2CH_3$ oxidation at 600 K with the corresponding fits to a breakdown of individual components. The solid red curve in Figure 3(a) represents a fit to the experimental data (open symbols) recorded at *m/z* 61.061 obtained with a weighted contribution of the experimentally measured photoionization spectra of undeuterated acetone, propanal, and methyloxirane. Adjusting the scaling factors for the photoionization cross-sections of these three isomers yields 62 % acetone-d_3, 20 % methyloxirane-d_3, and 18 % propanal-d_3. The photoionization spectrum recorded at *m/z* 46.005 shown in Figure 3(b) is similar to the absolute photoionization spectrum of formic acid (red solid curve) and consequently corresponds to formic acid-d_0. A small fraction of acetone-d_2 and formic acid-d_1 are also detected and are attributed to either deuterium exchange or additional reaction channels that do not proceed through a Korcek decomposition mechanism (see Table 1). This observation is in agreement with the observation of signals corresponding to formic acid and acetone in Figure 2 in a temperature region where the KHP signal reaches its maximum.

Because an absolute photoionization cross section for KHP is unavailable, the branching ratios of the formic acid-d_0 + acetone-d_3 Korcek pair are reported relative to the total concentration of experimentally measured 1- and 2-butene, see Table 1. Errors in the reported branching ratios

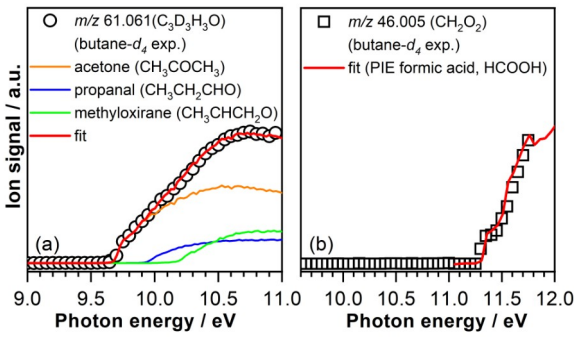

Figure 3. Photoionization identification of the oxidation products recorded at a) *m/z* 61.061 (CH_3D_3O) and b) *m/z* 46.005 in the JSR experiment at 600 K and 1 atm using isotopically labeled *n*-butane-d_4. The open symbols in panel (a) represent the measured data, while the solid red line shows the fit to the data constructed by adding the weighted contributions of the experimentally measured photoionization spectra of undeuterated acetone (orange line),[16] propanal (blue line),[17] and methyloxirane (green line). The open symbols in panel (b) represent the measured data while the red solid curve corresponds to measured photoionization spectra of formic acid.[16]

Table 1: Branching ratios, relative to the sum of butenes for the *n*-butane-$d_4 + O_2$ reaction, investigated in the JSR experiment at 600 K and 740 Torr. Stated uncertainties are based on statistical 1σ-uncertainties only.

Product $(CH_3(CD_2)_2CH_3)$ Exp.[a]	Mass [*m*/*z*]	Branching ratio
1-butene-d_3	59.081	0.75 ± 0.09
2-butene-d_2	58.075	0.25 ± 0.02
formic acid-d_0	46.005	0.87 ± 0.09
formic acid-d_1	47.011	0.46 ± 0.08
acetone-d_3	61.061	0.88 ± 0.09
acetone-d_2	60.054	0.11 ± 0.04

[a] Branching ratios relative to species other than the sum of butenes can be obtained by dividing the corresponding values relative to the sum of butenes.

due to deuterium exchange are estimated to be about 10 % based on the ratio between the butene expected to form in the butane-d_4 oxidation experiment, i.e. butene-d_3 and butene-d_2, and the small amount of butene that can only be explained as a result of deuterium exchange, i.e. butene-d_4 and butene-d_1. A substantial fraction of the acids and acetones formed in low- temperature *n*-butane oxidation may arise from Korcek decomposition of KHP, although the presence of a smaller fraction of formic acid-d_1 and acetone-d_2 (see Table 1) implies that not all formic acid and acetone arise from this channel. The JSR experiments show formation of KHP and demonstrate production of a characteristic pair of isotopically labelled products of Korcek decomposition. Experimental bounds on the rate coefficient for Korcek decomposition are required to constrain its possible effect on autoignition. Complementary laser photolysis experiments, in which the production of R radicals is initiated by photolytically generated Cl-atoms and subsequent reaction with *n*-butane, are used to better isolate the KHP decomposition step. These time-resolved product formation measurements, because of the shorter reaction times, are sensitive to a smaller set of reactions than are the JSR experiments. Figure 4 shows time-resolved signals from Cl-initiated undeuterated *n*-butane oxidation experiments performed at 600 K and 1690 Torr using MPIMS detection. The time evolution of the signals is displayed up to 72 ms, since for longer reaction times the evolution of the signals will be increasingly influenced by the chain propagation from OH produced during the initial steps of the oxidation reaction. Table S1 lists branching ratios of acetone/formic acid Korcek pair relative to the sum of 1- and 2-butene measured in the MPIMS experiment. The signal from the butenes, primary products of *n*-butyl + O_2 reactions,[18] rises on the timescale of the $R + O_2$ reaction and is closely followed by the rise of KHP under these high-pressure conditions.[9] Also shown in Figure 4 are formic acid and acetone signals (i.e. a Korcek pair). These signals have a common time behaviour, rising approximately with the decay of KHP, consistent with tertiary product formation.

The formation and decomposition of KHP and formation kinetics of acetone and formic acid were simulated (see Figure 4) using the AramcoMech 3.0 kinetic model[19] modified to include new KHP decomposition pathways (see

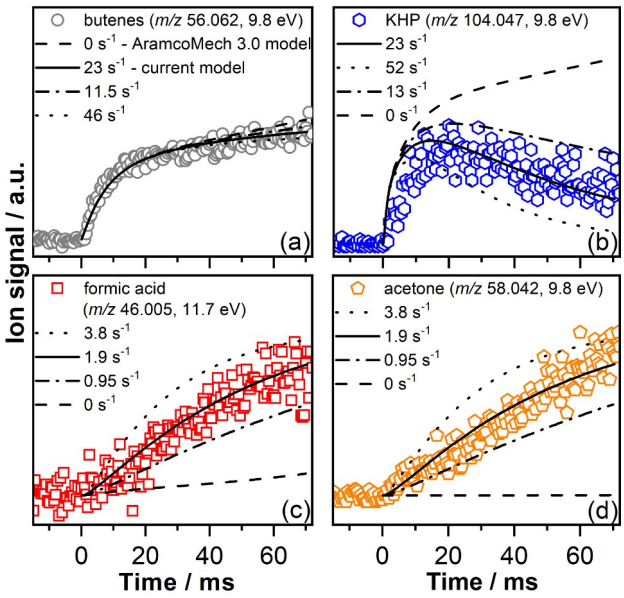

Figure 4. Time-resolved signals from the photolytic Cl-atom initiated *n*-butane oxidation measurements at 600 K, 1690 Torr, and $[O_2] = 5.3 \times 10^{18}$ cm^{-3} using high-pressure reactor interfaced with MPIMS. At 11.7 eV formic acid is the only isomer detected at *m*/*z* 46.005 and at 9.8 eV acetone is the only isomer detected at *m*/*z* 58.042. Model simulations and sensitivity analysis were performed using a modification of the AramcoMech 3.0 kinetic model, see text for details. The solid line shows the "best fit" estimates for rate coefficients, and the dotted and dot-dashed lines show effects of increasing and decreasing this estimate by factors of two (see Section 2 in Supporting Information for more details).

Section 2 in Supporting Information). In the model and in the underlying theoretical calculations, oxygen molecules are considered to be triplets. Excited O_2 (i.e., singlet) does not play a role under our experimental conditions. Modeling the decay of KHP in time requires addition of a phenomenological non-chain-branching removal pathway, as shown by the "0 s^{-1}" line in Figure 4(b), which does not include a non-chain branching removal. A net additional loss rate coefficient of 23 s^{-1} gives a good fit to the data. However, the model slightly overestimates the rate of KHP formation.

The part of this phenomenological removal that is the unimolecular decay of KHP to $HCOOH + CH_3COCH_3$ can be constrained via the measured yield of formic acid. Matching the formic acid yield requires the Korcek decomposition to have a rate coefficient of 1.9 s^{-1} at 600 K (see Figure 4c), which is a small fraction of the overall KHP removal. Strictly speaking, this is an upper limit for the rate coefficient, because other reactions may contribute to formic acid production, including wall reactions. A brute-force sensitivity analysis is provided in Supporting Information (see Section 3), propagating uncertainty in various *n*-butane oxidation reactions (e.g., hydrogen abstraction, RO_2 concerted elimination, $O_2 + QOOH$, $RO_2 + RO_2$, and KHP decomposition) to establish the uncertainty in the derived Korcek decomposition rate coefficient.

Although catalytic effects of acids may reduce the cyclization barrier,[5] experimental concentrations even of

the photolytic precursor are ≈500 times smaller than the acid concentrations employed by Jalan et al., so catalytic effects are likely to be negligible in the present case. The observed Korcek component is a small fraction (about 6.4 %) of total KHP removal in these conditions. However, the current estimated upper bound is about 10 times larger than a computational value, 0.16 s^{-1}, obtained at 600 K by Ranzi et al.,[12] in which cyclization is assumed to be the rate-limiting step. Even the estimated lower limit of the reaction rate constant of 0.95 s^{-1}, determined by comparing the experimental data with the modeled data is way above the value reported by Ranzi et al. This observation is consistent with the other results reported by Ranzi et al., which had to increase the Korcek reaction rate constant in *n*-heptane oxidation kinetic model by a factor of three to predict acetic and propanoic acid formation observed experimentally.[12,20] The Korcek reactions were also included in an *n*-pentane kinetic model to predict acetic acid concentration observed at 1 and 10 atm in a JSR.[21] The acetic acid concentration was significantly underestimated, even when the rate constant of the Korcek reaction calculated by Jalan et al.[5] was increased by a factor of 10.

The major new results of this work are evidence for the observation of a Korcek pair in oxidation of isotopically labeled *n*-butane and an experimental constraint on the rate coefficient for gas-phase Korcek decomposition. The Korcek mechanism is a substantial fraction of the organic acid production, but it is unlikely to be a significant perturbation on the autoignition process. The results provide experimental and computational bounds that enable the construction of more realistic and accurate kinetic mechanisms for autoignition chemistry.

The jet-stirred reactor utilized in the experiments is based on the design of Dagaut et al.,[22] slightly modified to accommodate direct sampling into TOF-MBMS.[23] The pressure of the experiments was set to near 1 atm (≈740 Torr), temperature was scanned from about 570–640 K, and the residence time inside of the 33.5 cm^3 reactor was 3.4 s. The high pressure laser photolysis reactor[9] that interfaces with the MPIMS[15] is an Inconel flow cell with inner dimensions of 0.5 cm diameter by 4 cm long. Both experiments utilize vacuum ultraviolet (VUV) photons from the Chemical Dynamics Beamline of the Advanced Light Source[24] to measure photoionization spectra of product species. Detailed information about the experimental setups and the methods used in the current investigation are provided in the Supporting Information (see Section 1).

Acknowledgements

This material is based upon work supported by the U.S. Department of Energy (DOE), Office of Science, Office of Basic Energy Sciences. The Lawrence Berkeley National Laboratory researchers were supported under contract no. DE-AC02-05CH11231, the gas phase chemical physics program through the Chemical Sciences Division of Lawrence Berkeley National Laboratory. Sandia National Laboratories is a multi-mission laboratory managed and operated by National Technology and Engineering Solutions of Sandia, LLC, a wholly owned subsidiary of Honeywell International, Inc., for the USDOE's National Nuclear Security Administration under contract DE-NA0003525. This paper describes objective technical results and analysis. Any subjective views or opinions that might be expressed in the paper do not necessarily represent the views of the USDOE or the United States Government. L.S. was supported as part of the Argonne-Sandia Consortium in High-Pressure Combustion Chemistry. The KAUST researchers were supported by competitive research funding from the King Abdullah University of Science and Technology. Argonne National Laboratory is supported by the U.S. Department of Energy, Office of Science, Office of Basic Energy Sciences, Division of Chemical Sciences, Geosciences, and Biosciences, under Contract DE-AC02-06CH11357. D.M.P.-V. acknowledges financial support provided by the UCF through the Seed Funding Program and the technical support by James Breen, Erik Granlund, and William Thur during the designing and fabrication of the JSR system. P. D. has received funding from the European Research Council under the European Community's Seventh Framework Programme (FP7/2007-2013)/ERC grant agreement No. 291049-2G-CSafe.

Conflict of Interest

The authors declare no conflict of interest.

Data Availability Statement

The data that support the findings of this study are available from the corresponding author upon reasonable request.

Keywords: Autoignition · Hydrocarbon Oxidation · Ketohydroperoxides · Korcek Reaction · Photoionization

[1] D. K. Manley, A. McIlroy, C. A. Taatjes, *Phys. Today* **2008**, *61*, 47–52.
[2] J. Zádor, C. A. Taatjes, R. X. Fernandes, *Prog. Energy Combust. Sci.* **2011**, *37*, 371–421.
[3] R. W. Walker, C. Morley, in *Comprehensive Chemical Kinetics, Vol. 35* (Ed.: M. J. Pilling), Elsevier, Amsterdam, **1997**, pp. 1–124.
[4] a) R. K. Jensen, S. Korcek, M. Zinbo, M. D. Johnson, *Int. J. Chem. Kinet.* **1990**, *22*, 1095–1107; b) R. K. Jensen, S. Korcek, L. R. Mahoney, M. Zinbo, *J. Am. Chem. Soc.* **1981**, *103*, 1742–1749; c) R. K. Jensen, S. Korcek, L. R. Mahoney, M. Zinbo, *J. Am. Chem. Soc.* **1979**, *101*, 7574–7584; d) E. J. Hamilton, S. Korcek, L. R. Mahoney, M. Zinbo, *Int. J. Chem. Kinet.* **1980**, *12*, 577–603.
[5] A. Jalan, I. M. Alecu, R. Meana-Paneda, J. Aguilera-Iparraguirre, K. R. Yang, S. S. Merchant, D. G. Truhlar, W. H. Green, *J. Am. Chem. Soc.* **2013**, *135*, 11100–11114.
[6] K. Moshammer, A. W. Jasper, D. M. Popolan-Vaida, A. Lucassen, P. Diévart, H. Selim, A. J. Eskola, C. A. Taatjes, S. R. Leone, S. M. Sarathy, Y. Ju, P. Dagaut, K. Kohse-Höinghaus, N. Hansen, *J. Phys. Chem. A* **2015**, *119*, 7361–7374.

[7] a) N. Blin-Simiand, F. Jorand, K. Sahetchian, M. Brun, L. Kerhoas, C. Malosse, J. Einhorn, *Combust. Flame* **2001**, *126*, 1524–1532; b) F. Jorand, A. Hess, O. Perrin, K. Sahetchian, L. Kerhoas, J. Einhorn, *Int. J. Chem. Kinet.* **2003**, *35*, 354–366; c) K. A. Sahetchian, R. Rigny, S. Circan, *Combust. Flame* **1991**, *85*, 511–514.

[8] F. Battin-Leclerc, O. Herbinet, P.-A. Glaude, R. Fournet, Z. Zhou, L. Deng, H. Guo, M. Xie, F. Qi, *Angew. Chem. Int. Ed.* **2010**, *49*, 3169–3172; *Angew. Chem.* **2010**, *122*, 3237–3240.

[9] A. J. Eskola, O. Welz, J. Zador, I. O. Antonov, L. Sheps, J. D. Savee, D. L. Osborn, C. A. Taatjes, *Proc. Combust. Inst.* **2015**, *35*, 291–298.

[10] a) F. Battin-Leclerc, A. Rodriguez, B. Husson, O. Herbinet, P.-A. Glaude, Z. Wang, Z. Cheng, F. Qi, *J. Phys. Chem. A* **2014**, *118*, 673–683; b) Z. Wang, O. Herbinet, N. Hansen, F. Battin-Leclerc, *Prog. Energy Combust. Sci.* **2019**, *73*, 132–181; c) J. C. Davis, A. L. Koritzke, R. L. Caravan, I. O. Antonov, M. G. Christianson, A. C. Doner, D. L. Osborn, L. Sheps, C. A. Taatjes, B. Rotavera, *J. Phys. Chem. A* **2019**, *123*, 3634–3646; d) I. O. Antonov, J. Zádor, B. Rotavera, E. Papajak, D. L. Osborn, C. A. Taatjes, L. Sheps, *J. Phys. Chem. A* **2016**, *120*, 6582–6595; e) L. Sheps, A. L. Dewyer, M. Demireva, J. Zádor, *J. Phys. Chem. A* **2021**, *125*, 4467–4479.

[11] C. F. Goldsmith, M. Burke, Y. Georgievskii, S. J. Klippenstein, *Proc. Combust. Inst.* **2015**, *35*, 283–290.

[12] E. Ranzi, C. Cavallotti, A. Cuoci, A. Frassoldati, M. Pelucchi, T. Faravelli, *Combust. Flame* **2015**, *162*, 1679–1691.

[13] a) K. Kawamura, L. L. Ng, I. R. Kaplan, *Environ. Sci. Technol.* **1985**, *19*, 1082–1086; b) E. Zervas, X. Montagne, J. Lahaye, *Environ. Sci. Technol.* **2001**, *35*, 2746–2751; c) E. Zervas, X. Montagne, J. Lahaye, *Atmos. Environ.* **2001**, *35*, 1301–1306; d) B. G. Bunting, C. B. Wildman, J. P. Szybist, S. Lewis, J. Storey, *Int. J. Engine Res.* **2007**, *8*, 15–27.

[14] O. Herbinet, F. Battin-Leclerc, S. Bax, H. L. Gall, P.-A. Glaude, R. Fournet, Z. Zhou, L. Deng, H. Guo, M. Xie, F. Qi, *Phys. Chem. Chem. Phys.* **2011**, *13*, 296–308.

[15] D. L. Osborn, P. Zou, H. Johnsen, C. C. Hayden, C. A. Taatjes, V. D. Knyazev, S. W. North, D. S. Peterka, M. Ahmed, S. R. Leone, *Rev. Sci. Instrum.* **2008**, *79*, 104103.

[16] T. A. Cool, J. Wang, K. Nakajima, C. A. Taatjes, A. McLlroy, *Int. J. Mass Spectrom.* **2005**, *247*, 18–27.

[17] J. Wang, B. Yang, T. A. Cool, N. Hansen, T. Kasper, *Int. J. Mass Spectrom.* **2008**, *269*, 210–220.

[18] A. J. Eskola, O. Welz, J. D. Savee, D. L. Osborn, C. A. Taatjes, *J. Phys. Chem. A* **2013**, *117*, 12216–12235.

[19] C.-W. Zhou, Y. Li, U. Burke, C. Banyon, K. P. Somers, S. Ding, S. Khan, J. W. Hargis, T. Sykes, O. Mathieu, E. L. Petersen, M. AlAbbad, A. Farooq, Y. Pan, Y. Zhang, Z. Huang, J. Lopez, Z. Loparo, S. S. Vasu, H. J. Curran, *Combust. Flame* **2018**, *197*, 423–438.

[20] M. Pelucchi, M. Bissoli, C. Cavallotti, A. Cuoci, T. Faravelli, A. Frassoldati, E. Ranzi, A. Stagni, *Energy Fuels* **2014**, *28*, 7178–7193.

[21] J. Bugler, A. Rodriguez, O. Herbinet, F. Battin-Leclerc, C. Togbé, G. Dayma, P. Dagaut, H. J. Curran, *Proc. Combust. Inst.* **2017**, *36*, 441–448.

[22] P. Dagaut, M. Cathonnet, J. P. Rouan, R. Foulatier, A. Quilgars, J. C. Boettner, F. Gaillard, H. James, *J. Phys. E: Sci. Instrum.* **1986**, *19*, 207.

[23] a) F. N. Egolfopoulos, N. Hansen, Y. Ju, K. Kohse-Höinghaus, C. K. Law, F. Qi, *Prog. Energy Combust. Sci.* **2014**, *43*, 36–67; b) N. Hansen, T. A. Cool, P. R. Westmoreland, K. Kohse-Hoinghaus, *Prog. Energy Combust. Sci.* **2009**, *35*, 168–191.

[24] a) P. A. Heimann, M. Koike, C. W. Hsu, D. Blank, X. M. Yang, A. G. Suits, Y. T. Lee, M. Evans, C. Y. Ng, C. Flaim, H. A. Padmore, *Rev. Sci. Instr.* **1997**, *68*, 1945–1951; b) S. R. Leone, M. Ahmed, K. R. Wilson, *Phys. Chem. Chem. Phys.* **2010**, *12*, 6564–6578.

Manuscript received: June 22, 2022
Accepted manuscript online: July 27, 2022
Version of record online: September 14, 2022